MOLECULAR AND CELLULAR BIOLOGY, May 2009, p. 2419–2430 Vol. 29, No. 9
0270-7306/09/$08.00+0 doi:10.1128/MCB.01050-08

Nucleosome Remodeling and Transcriptional Repression Are Distinct Functions of Isw1 in *Saccharomyces cerevisiae*[▽]

Marina Pinskaya,[1,2] Anitha Nair,[1] David Clynes,[1] Antonin Morillon,[2] and Jane Mellor[1]*

Department of Biochemistry, University of Oxford, South Parks Road, Oxford OX1 3QU, United Kingdom,[1] and Centre de Génétique Moléculaire, CNRS, Gif-sur-Yvette, France[2]

Received 4 July 2008/Returned for modification 7 August 2008/Accepted 16 February 2009

The SANT domain is a nucleosome recognition module found in transcriptional regulatory proteins, including chromatin-modifying enzymes. It shows high functional degeneracy between species, varying in sequence and copy number. Here, we investigate functions in vivo associated with two SANT motifs, SANT and SLIDE, in the *Saccharomyces cerevisiae* Isw1 chromatin-remodeling ATPase. We show that differences in the primary structures of the SANT and SLIDE domains in yeast and *Drosophila melanogaster* reflect their different functions. In yeast, the SLIDE domain is required for histone interactions, while this is a function of the SANT domain in flies. In yeast, both motifs are required for optimal association with chromatin and for formation of the Isw1b complex (Isw1, Ioc2, and Ioc4). Moreover, nucleosome remodeling at the *MET16* locus is defective in strains lacking the SANT or SLIDE domain. In contrast, the SANT domain is dispensable for the interaction between Isw1 and Ioc3 in the Isw1a complex. We show that, although defective in nucleosome remodeling, Isw1 lacking the SANT domain is able to repress transcription initiation at the *MET16* promoter. Thus, chromatin remodeling and transcriptional repression are distinct activities of Isw1.

In eukaryotic organisms, DNA is folded into a highly compacted chromatin structure. This packing restricts the accessibility of DNA to various nuclear factors involved in DNA-templated processes, including transcription. There are several mechanisms that regulate chromatin structure, among them covalent modifications of histones provided by histone-modifying enzymes and disruption of histone-DNA interactions by ATP-dependent chromatin-remodeling enzymes. Although these two classes of chromatin-modifying factors are functionally distinct, their subunits share conserved motifs, such as the chromodomain, bromodomain, plant homeodomain finger, and SANT domain (56). These domains are involved in histone tail recognition and binding, thus providing recruitment of these enzymes to targeted regions within the chromatin. The bromodomain shows highly selective binding to acetylated lysines (24, 25, 47). The chromodomain and plant homeodomain finger bind to methylated lysines (17, 27, 28, 34–36, 39, 49). In each case, the specific binding is defined by a hydrophobic pocket, formed by aromatic residues and surrounded by residues determining the specificity of binding.

In contrast, our understanding of the function of the SANT domain is still restricted to examples that often prove to be protein specific. Historically, the SANT domain was identified based on its homology to the DNA-binding domain of c-Myb (1). It consists of three alpha-helices arranged in a helix-turn-helix motif; each helix contains a conserved, bulky aromatic residue that plays a key role in helix packing. Although structurally similar, the SANT domain and the canonical Myb DNA-binding domain are functionally divergent (21, 26, 48). The DNA-contacting residues in Myb are not conserved in SANT and often prove to be incompatible with DNA interaction. The lack of conservation between SANT domains together with the variation in sequence and copy number suggests a high functional divergence. In *Saccharomyces cerevisiae*, the SANT domain is broadly present among ATP-dependent chromatin-remodeling enzymes and their complexes (Swi3p from SWI/SNF, Rsc8p from RSC, and Isw1 and Isw2p from ISWI), as well as among transcription factors (Bas1p, Tfc5p, and Tbf1p) and protein components of histone acetyltransferase (HAT) and histone deacetylase complexes (Ada2p and Snt1p) (1, 4, 5, 22, 54). In yeast and other species, the SANT domain has been shown to be essential for protein function, providing protein-histone interactions or determining the integrity and activity of complexes (15, 42, 61).

Paired SANT motifs are found in the *Drosophila melanogaster* chromatin-remodeling ATPase ISWI protein (DmISWI) and its *S. cerevisiae* homologues Isw1 and Isw2. DmISWI contains two closely spaced SANT motifs at its carboxyl terminus. The downstream SANT motif, named SLIDE (SANT-like ISWI domain), contains considerable sequence insertions and replacements compared to the canonical SANT domain. Together, SANT and SLIDE domains comprise a nucleosome recognition module, playing different roles in nucleosome recognition and enzyme activity in vitro (21). Based on crystallographic and biochemical data, the SLIDE domain of DmISWI is proposed to be crucial for DNA binding and for the ATPase activity of the enzyme. Grune et al. suggest that the SLIDE domain is likely to interact with the major groove of the DNA closest to the N-terminal tail of H4, allowing direct interactions between the C-terminal region of DmISWI and H4 tail residues within the nucleosome (21). A patch of basic residues on histone H4, which are positioned 1.5 turns on either side of the entry/exit site for the nucleosomal DNA (16), are required for nucleosome remodeling by DmISWI (8). Significantly, acety-

* Corresponding author. Mailing address: Department of Biochemistry, University of Oxford, South Parks Road, Oxford OX1 3QU, United Kingdom. Phone: 44 1865 275303. Fax: 44 1865 275297. E-mail: jane.mellor@bioch.ox.ac.uk.

▽ Published ahead of print on 9 March 2009.

lation of H4, particularly H4K16 and H4K12, reduces the ability of DmISWI to interact productively with H4 (9, 11). By contrast, the SANT domain is proposed to be involved in H3 histone binding or presentation (21). Both domains are essential for the nucleosome-stimulated ATPase activity of DmISWI in vitro.

Another extensive study was performed on the role of the SANT-containing C-terminal part of the Isw2 chromatin-remodeling ATPase in its docking to nucleosomal and extranucleosomal DNA (13, 14). Here, it was proposed that the ATPase domain (DEXD lobe) interacts with the internal site of the nucleosome for translocation along DNA whereas the HAND, SANT, spacer, and SLIDE domains within the C-terminal part of Isw2 form contacts with the nucleosome entry/exit site and the extranucleosomal DNA, allowing efficient anchoring of the protein, its proper orientation, and directional nucleosome movement.

These markedly different interpretations of SANT domain function within the related family of ATPases called our attention to the yeast Isw1 protein, also containing two closely spaced SANT motifs in its carboxyl terminus. Isw1 is the ATPase subunit of the Isw1a and Isw1b chromatin-remodeling complexes. Under stressful conditions, Isw1 shows redundancy with Isw2 and Chd1 chromatin-remodeling factors (57), although individually the activity of Isw1 is promoter context dependent, leading to both derepression and deactivation of transcription (32, 37, 43, 59, 60). Recent data suggest that Isw1 functions in collaboration with the NuA4 HAT complex and the Swr1 histone replacement complex to establish an appropriate chromatin structure genomewide and specifically repress TATA-containing stress-responsive genes (37). Moreover, at some TATA-containing genes, Isw1 is proposed to repress the release of RNA polymerase II (RNAPII) from the promoter at the postinitiation stage of transcription (44, 45). In neither of these studies was the role of the catalytic activity of Isw1 in transcriptional repression determined, so it is not known whether repression results from nucleosome positioning or protein-protein interactions involving Isw1 or both. The Ioc (*I*sw *o*ne *c*omplex) proteins, which modulate Isw1 remodeling activity in vitro, also give distinct functions to Isw1 complexes in vivo (18, 44, 45, 55, 59, 60). According to the existing models, the Isw1a complex (Isw1/Ioc3) is implicated in repression at initiation while the Isw1b complex (Isw1/Ioc2/Ioc4) coordinates transcription elongation and termination (40, 44, 45, 60). In addition, Isw1 is proposed to be involved in silencing of the ribosomal DNA loci independently of Ioc proteins (46) and of the *HMR* mating-type locus, where Ioc3 functions redundantly with its homologue Esc8 (12).

Isw1 shares 48% homology with the carboxyl terminus of DmISWI, although it differs remarkably in the distribution of charged amino acid residues within this region. The question we addressed in this study was whether the SANT and SLIDE domains of Isw1 are essential for nucleosome binding and protein activity, focusing our attention on in vivo aspects of Isw1 function in transcription regulation. We show that differences in the primary structures of SANT and SLIDE domains in two species, *S. cerevisiae* and *D. melanogaster*, reflect different functions. Together, the Isw1 SANT and SLIDE domains provide optimal protein anchoring to nucleosomes, with the SLIDE domain required for histone interactions. Moreover, nucleosome remodeling is defective in strains lacking the SANT or SLIDE domain. Unexpectedly, we found that repression of transcription by Isw1 takes place even when the SANT domain is deleted, although this form of Isw1 is incapable of remodeling nucleosomes. The SANT domain is not required for Isw1 and Ioc3 interactions (Isw1a), their recruitment to chromatin, or their role to impede TATA-binding protein (TBP) and RNAPII binding resulting in repression of transcription. We conclude that the C-terminal domain of Isw1 confers a repressive function in the form of Isw1a, which is independent of the chromatin-remodeling activity of Isw1.

MATERIALS AND METHODS

Construction of Isw1 deletion derivatives. Wild-type (WT) Isw1 and its catalytic mutant, $Isw1_{K227R}$, were recovered from the BMA64 and YTT1223 strains (3, 57) by homologous recombination using linearized pRS306-containing sequences homologous to the *ISW1* flanking sequences to give rise to plasmids pRS306-Isw1 and pRS306-K227R, respectively. Isw1 deletion derivatives, lacking SANT or SLIDE, were constructed by a two-step PCR strategy as described in reference 21, using a high-fidelity *Pfu* polymerase (Promega). Mutagenic regions were cloned into pRS306-Isw1, giving rise to plasmids pRS306-SANT and pRS306-SLIDE. The SANT domain (amino acids [aa] 881 to 933) was replaced with the sequence GGGGG and the SLIDE domain (aa 987 to 1050) with the sequence GGSRG. The identity of the clones was verified by sequence analysis.

Strains and media. Manipulations of strains were done according to standard procedures. All strains used in this study are congenic to W303-1B, except for the *trp1* deletion, and are listed in Table 1. Strains expressing deletion derivatives were obtained by integration of SANT, SLIDE, and the K227R mutant from appropriate plasmids at the *ISW1* genomic locus, using the standard *URA3* pop-in/5-fluoroorotic acid pop-out method. N- and C-terminal truncation of Isw1 (aa 1 to 743 and 881 to 1129, respectively), epitope tagging, and gene deletions were done by a single-step gene replacement or sequence insertion using PCR-generated DNA fragments (38). Hemagglutinin (HA)-tagged TBP was generated as previously described (33). Appropriate targeting of disruption cassettes and epitope tagging were confirmed by PCR and Western blotting, respectively. For most experiments detailed below, strains were grown in yeast extract-peptone-dextrose or methionine-depleted Hartwell's complete medium to a density of 1×10^7 to 1.5×10^7 cells/ml at 30°C. Otherwise, yeast was cultured in yeast-peptone-2% glucose or yeast-peptone-2% galactose to the same density.

Immunoprecipitations. The antibodies used in this study were Myc and peroxidase antiperoxidase (Sigma); HA (Santa Cruz); horseradish peroxidase-conjugated Myc, H3, and H4 (Upstate); H3K4me1, -me2, and -me3 (Abcam); H4S1ph (Abcam); and H2BS1ph and H4S1ph (Millipore). Coimmunoprecipitation was done from 2 liters of culture as described previously (59). Cells were resuspended in 5 ml of buffer A containing 150 mM NaCl, broken by passing several times through the French press. Cell extract was clarified by centrifugation at $10^4 \times g$ for 10 min at 4°C. One milliliter of each extract was incubated with an appropriate antibody for 2 to 12 h, followed by protein A–Sepharose CL-4B, immunoglobulin G-Sepharose (Amersham), or glutathione-Sepharose 4B (Pharmacia) for 90 min at 4°C. Beads were pelleted at $500 \times g$ and washed three times with ice-cold buffer A containing 150 mM NaCl. Immunoprecipitates were eluted by boiling in Laemmli sodium dodecyl sulfate loading buffer for 10 min. Samples of the whole-cell extract, immunoprecipitates, and supernatants were run on a 12% sodium dodecyl sulfate-polyacrylamide gel electrophoresis gel, transferred to nitrocellulose, probed with the appropriate antibodies, and visualized with Pico or Femto chemiluminescent substrate (Pierce).

Chromatin immunoprecipitation was performed as described previously (41, 44) with the following modifications. Proteins were cross-linked to chromatin at room temperature for 30 min. The reaction was stopped by the addition of glycine to a final concentration of 0.5 M. Cells were broken with glass beads on a MagNA Lyser (Roche) and subjected to sonication at 4°C using a Haake C25P sonicator (Thermo Electron Corporation) for 30 min to achieve 300-bp DNA fragmentation. The sonicated lysate was clarified by centrifugation at 13,000 rpm for 10 min. The sonicated extract was incubated with antibodies overnight and with beads for 2 h. Immunoprecipitated DNA was purified using a Qiagen PCR purification kit and amplified by real-time PCR on Rotor Gene 6000 (Corbett) or LightCycler480 (Roche) with primers to promoter and coding regions of different genes (available on request). Error bars in the figures reflect standard deviations of an average signal obtained from at least three independent experiments. In the case of TBP and RNAPII chromatin immunoprecipitation (ChIP),

TABLE 1. Strains used in this study[a]

Strain(s)	Background	Reference
BMA64	*MATα ura3-1 ade2-1 his3-11,5 trp1Δ leu2-3,112 can1-100*	3
YTT1223	*MAT***a** $isw1_{K227R}$	57
MP1	*isw1*::*URA3*	This study
MP2	*isw1Δ2641-2799* (SANT, aa 881–933)	This study
MP3	*isw1Δ2961-3150* (SLIDE, aa 987–1050)	This study
MP4	*isw1Δ2641-3150* (248 C-terminal amino acids)	This study
MP5–MP7	Same as MP2–MP4 but *ISW1-3′ 13MYC*::*kanMX*	This study
MP8	*Pgal 5′TAP-ISW1Δ1-2229*::*HIS3*	This study
MP9–MP11	Same as MP2–MP4 but *ISW1-3′TAP*::*URA3*	This study
MP12–MP14	Same as MP2–MP4 but *isw2*::*HIS3 chd1*::*kanMX*	This study
MP15–MP18	Same as MP1–MP4 but *IOC2-13MYC*::*kanMX*	This study
MP19–MP22	Same as MP1–MP4 but *IOC3-13MYC*::*kanMX*	This study
MP23–MP26	Same as MP1–MP4 but *IOC4-13MYC*::*kanMX*	This study
MP27–MP29	Same as MP2–MP4 but *ISW1-3′TAP*::*URA3 IOC2-13MYC*::*kanMX*	This study
MP30–MP32	Same as MP2–MP4 but *ISW1-3′TAP*::*URA3 IOC3-13MYC*::*kanMX*	This study
MP33–MP35	Same as MP2–MP4 but *ISW1-3′TAP*::*URA3 IOC4-13MYC*::*kanMX*	This study
MP36	*Pgal 5′GST-ISW1Δ1-2229*::*HIS3*	This study
MP37	Same as MP34 but *IOC3-13MYC*::*kanMX*	This study
MP38	Same as MP34 but *IOC4-13MYC*::*kanMX*	This study
MP39	*MATα ura3-1 ade2-1 his3-11,5 trp1-1 leu2-3,112 can1-100 SPT15-3HA*	This study
MP40–MP42	Same as MP1–MP3 but *SPT15-3HA*	This study
MP43	Same as MP2 but also $isw1_{K227R}$	This study
MP44	Same as MP3 but also $isw1_{K227R}$	This study
MP45	*MATα ura3-1 ade2-1 his3-11,5 trp1-1 leu2-3,112 can1-100* $isw1_{K227R}$	This study

[a] All MP strains were derived from BMA64.

the occupancy values are normalized to the signal at tF(GAA)P2 (tRNAPhe region in chromosome XVI, coordinates 622628 to 622537). For other experiments, values were normalized to an untagged control. The relative occupancy of each locus by the protein is presented as a percentage of input.

RNA analysis. Total RNA was prepared by hot acid-phenol extraction (29); 10 μg of RNA was separated on a 1.5% formaldehyde-MOPS (morpholinepropanesulfonic acid) agarose gel in a buffer containing formaldehyde, blotted, and sequentially hybridized to [α-^{32}P]dATP-labeled probe to the 5′-coding region of *MET16* mRNA and 18S rRNA. cDNA was generated by SuperScript II reverse transcriptase (Invitrogen) using poly(dN)$_6$ random hexamers (Roche) and oligo(dT)$_{23}$ primers (Sigma) and quantified by real-time PCR using a set of primers corresponding to a 200-bp fragment of the 5′-coding region of *MET16* and U4 snRNA. Error bars reflect standard deviations of an average signal obtained from three independent experiments.

MNase mapping. The micrococcal nuclease (MNase) method is based on a procedure described previously (30, 31, 44, 45). Chromatin was digested with 20 units/ml of MNase for 4 min.

Immunofluorescence microscopy. Immunofluorescence was performed as described previously (6). Cells expressing Myc-tagged proteins were grown to a mid-log phase and then fixed by adding formaldehyde directly to the cultures to a final concentration of 4.5% for 1 h. Cells were spheroplasted with 30 μl of 10 mg/ml Zymolyase 100T at room temperature for 15 min, washed twice with 1 M sorbitol, and incubated with antibodies, followed by two washes in phosphate-buffered saline. The primary antibody used was the mouse monoclonal anti-c-Myc antibody (1:75 dilution; Sigma) and anti-CBP antibody (1:75 dilution; Open Biosystems), and the secondary antibodies were Alexa Fluor 488 conjugated to goat anti-mouse or anti-rabbit immunoglobulin G (1:500 dilution; Molecular Probes). Nuclei were stained using DAPI (4′,6-diamidino-2-phenylindole) dye. Cells were visualized on a Zeiss Axioplan 2 imaging fluorescence microscope.

RESULTS

***S. cerevisiae* Isw1 contains SANT and SLIDE domains.** The C-terminal part of *S. cerevisiae* Isw1 contains two regions that share 48% homology with *D. melanogaster* SANT (DmSANT) and SLIDE (DmSLIDE) domains. We referred to the corresponding regions as yeast SANT (ySANT; aa 883 to 933) and SLIDE (ySLIDE; aa 988 to 1052) domains (Fig. 1). Analysis of the primary structures of two proteins showed that hydrophobic residues are well conserved or are conservatively substituted within the carboxyl terminus of Isw1, although basic residues present in DmSANT are substituted to acidic residues within ySANT and vice versa within ySLIDE. As a result, the surface charge distribution at the carboxyl terminus of Isw1 is reversed compared to that of DmISWI, the ySANT domain displays an overall positive charge, with a calculated pI value of 9.2, and the ySLIDE domain is negatively charged, with a calculated pI value of 5.2 (Fig. 1). Taken together, these observations suggested that ySANT and ySLIDE domains are

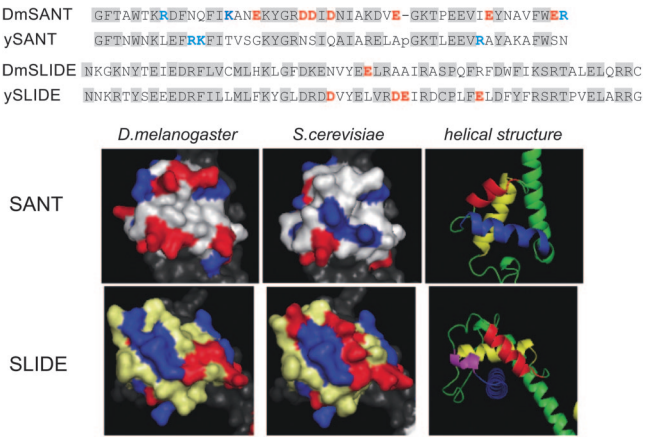

FIG. 1. *S. cerevisiae* Isw1 SANT and SLIDE domains. (A) Sequence alignment of the SANT and SLIDE domains of ISWI homologues from *D. melanogaster* (ISWI) and *S. cerevisiae* (Isw1). Conserved and conservatively substituted residues are in gray boxes; polarity changes are in boldface and red for Glu (E) and Asp (D) and blue for Lys (K) and Arg (R). The charge distributions in SANT and SLIDE are mapped with the use of PyMol software.

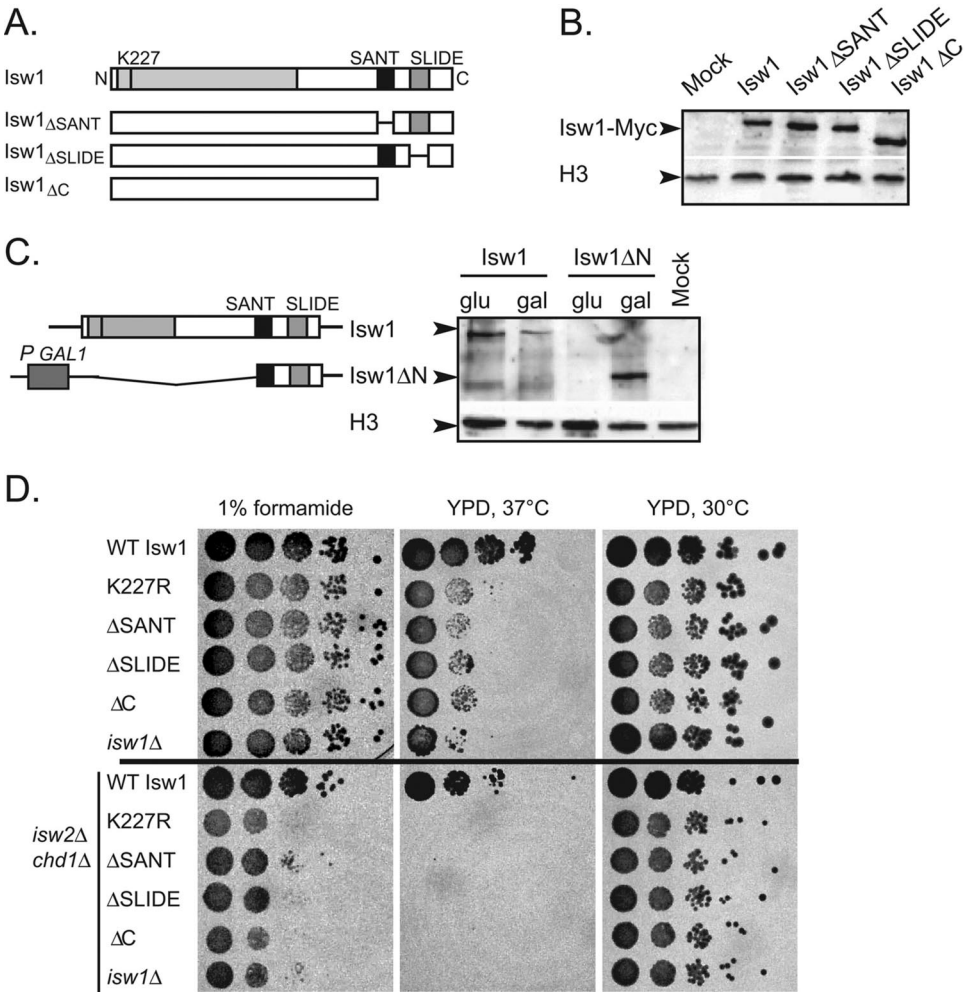

FIG. 2. Phenotypic characterization of derivatives of Isw1. (A) Deletion derivatives of Isw1 lacking SANT ($Isw1_{\Delta SANT}$), SLIDE ($Isw1_{\Delta SLIDE}$), or both domains ($Isw1_{\Delta C}$). For SANT and SLIDE proteins, a deleted domain was replaced by a polyglycine spacer. (B) Expression levels of Myc-tagged Isw1 deletion derivatives analyzed by Western blotting. (C) Expression levels of TAP-tagged WT Isw1 and $Isw1_{\Delta N}$ expressed from a galactose-inducible promoter and analyzed by Western blotting. (D) Results of temperature and formamide sensitivity growth assays showing 10-fold serial dilutions of the indicated strains, incubated for 3 days at 30°C unless indicated otherwise. glu, glucose; gal, galactose; YPD, yeast extract-peptone-dextrose.

structurally related to DmSANT and DmSLIDE but may differ remarkably in their nucleosome recognition functions. Particularly, the ySLIDE domain appears to be incompatible with a role in DNA binding, as was suggested for DmSLIDE. We aimed to determine the contribution of the SANT and SLIDE domains to Isw1 activity, focusing our attention on aspects of its in vivo function. For this purpose, we generated strains expressing WT Isw1, an ATPase-defective form of Isw1 with a substitution of K227R ($Isw1_{K227R}$), and derivatives lacking the SANT or SLIDE domain ($Isw1_{\Delta SANT}$ or $Isw1_{\Delta SLIDE}$, respectively) or lacking the 248 C-terminal amino acids including both the SANT and SLIDE domains ($Isw1_{\Delta C}$) (Fig. 2A). The three derivatives of Isw1 are expressed as stable proteins and to the same level as the WT (Fig. 2B). In addition, we generated a construct expressing the 248 C-terminal amino acids of Isw1 ($Isw1_{\Delta N}$) with a C-terminal tandem affinity purification (TAP) tag from the regulated *GAL1* promoter. When induced, this construct produced the C-terminal peptide at slightly higher levels than endogenous Isw1 with a C-terminal TAP tag (Fig. 2C).

$Isw1_{\Delta SANT}$ and $Isw1_{\Delta SLIDE}$ share phenotypes with Isw1Δ. Under stressful conditions, such as high temperature and the presence of formamide, Isw1 shows redundancy with Isw2 and Chd1 chromatin-remodeling factors (57). We combined $Isw1_{\Delta SANT}$, $Isw1_{\Delta SLIDE}$, or $Isw1_{\Delta C}$ with the *isw2*Δ and *chd1*Δ strains to determine whether the SANT and SLIDE domains are required for stress resistance (Fig. 2D). All combination failed to grow at high temperature, mimicking the *isw1*Δ *isw2*Δ *chd1*Δ strain. On plates containing formamide, however, the *chd1*Δ *isw2*Δ $ISW1_{\Delta SANT}$ strain showed more resistance than the *chd1*Δ *isw2*Δ $ISW1_{\Delta SLIDE}$ or *chd1*Δ *isw2*Δ $isw1_{\Delta C}$ strain, suggesting that the SANT and SLIDE domains might confer different properties to Isw1.

The C-terminal region of Isw1 is required for nuclear localization. To explore the cellular localization of Isw1 and its derivatives, we performed an immunofluorescence assay with

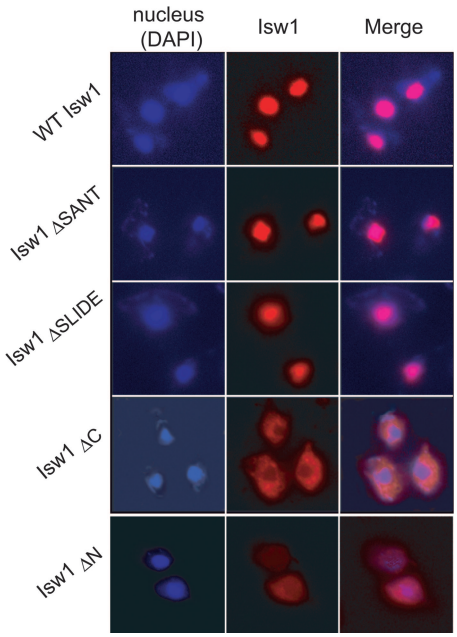

FIG. 3. The C-terminal part of Isw1 determines its nuclear localization. Immunofluorescence microscopy images of the derivatives of Isw1 indicated.

cells expressing Myc-tagged or TAP-tagged proteins (Fig. 3). We found that $Isw1_{\Delta SANT}$ and $Isw1_{\Delta SLIDE}$ localize to the nucleus like WT Isw1. In contrast, the $Isw1_{\Delta C}$ derivative is almost exclusively present in the cytoplasm, suggesting that a nuclear localization signal is located within the C-terminal region of the protein. To confirm this, we examined the localization of a peptide containing the 248 C-terminal amino acids of Isw1 ($Isw1_{\Delta N}$). This peptide is present in both the cytoplasm and the nucleus and indicates that the C-terminal region contains sequences sufficient to direct nuclear localization (Fig. 3). Thus, Isw1 is likely to contain sequences that determine its nuclear localization within the C-terminal region. The localization of $Isw1_{\Delta N}$, $Isw1_{\Delta SANT}$, and $Isw1_{\Delta SLIDE}$ to the nucleus allowed us to determine functions associated with these domains.

The C-terminal domain of Isw1 is sufficient for association with chromatin. The C-terminal domain of Isw1 ($Isw1_{\Delta N}$) is expressed as a TAP fusion from the galactose-inducible *GAL1* promoter. Given that when induced, at least a proportion of $Isw1_{\Delta N}$ is nuclear (Fig. 3), we asked whether this region of Isw1 is sufficient for association with chromatin by using the standard ChIP assay followed by real-time PCR at the locus of the *MET16* gene, whose transcription is regulated by Isw1 (45). First, we examined the association of full-length TAP-tagged Isw1 with *MET16*. As TAP-tagged Isw1 is expressed from its own promoter, it is expressed in both glucose and galactose. In glucose, it is recruited to *MET16* at both the 5′ and 3′ regions, with the highest levels at the 3′ open reading frame (ORF) region, although some of this signal may reflect Isw1 association with the promoter of *MRP2* close to the 3′ region of *MET16* (Fig. 4A). In galactose, the signals across *MET16* drop slightly, probably reflecting the lower overall levels of Isw1 in the cell (Fig. 2C). Next, we examined the association of $Isw1_{\Delta N}$ with *MET16*. When induced in galactose, $Isw1_{\Delta N}$ showed a profile of recruitment that was very similar to that seen in WT cells. Although the total levels of $Isw1_{\Delta N}$ are higher than those of WT Isw1 in galactose medium, a proportion of the protein is cytoplasmic and the nuclear concentration of $Isw1_{\Delta N}$ is likely to be lower than that of the WT (Fig. 3, compare top and bottom panels). In addition, we observed a low binding signal for both Isw1 and $Isw1_{\Delta N}$ at a control intergenic region (Fig. 4C and data not shown). Thus, the association we observe with *MET16* is unlikely to be explained by nonspecific association of $Isw1_{\Delta N}$ with chromatin. This suggests that the C-terminal domain of Isw1 is sufficient for recruitment to *MET16*. Next, we asked which regions within the C-terminal domain are required for Isw1 association with chromatin.

The SANT and SLIDE domains are required for optimal Isw1 association with chromatin. We addressed the role of the SANT and SLIDE domains in the recruitment of Isw1 to chromatin. ChIP followed by real-time PCR was performed on the *MET16* gene, which is induced when methionine is depleted from the medium (Fig. 4B) or at the induced *GAL1* locus (Fig. 4C). The signal obtained is normalized to that obtained using an untagged strain. No significant signal is observed at the *MET16* locus in the strain expressing $Isw1_{\Delta C}$, with both SANT and SLIDE deleted, most likely as a result of the mislocalization of the protein to the cytoplasm (Fig. 4B).

At the repressed *MET16* gene, full-length Isw1 is recruited to the 5′ and 3′ regions, with the highest levels at the 3′ ORF region (Fig. 4A and B). The association of $Isw1_{\Delta SANT}$ or $Isw1_{\Delta SLIDE}$ with repressed *MET16* is reduced at both the promoter and the 3′ ORF. We considered the possibility that loss of the SANT or SLIDE domain results in a form of Isw1 with relaxed specificity in its association with chromatin, resulting in a loss of *MET16* due to association elsewhere in the genome. We tested this by examining three additional loci: induced *GAL1*, the *FMP27* middle ORF, and an intergenic region from chromosome V in cells cultured in glucose (Fig. 4C). At both the *GAL1* upstream region and the 3′ ORF, association of WT Isw1 and $Isw1_{K227R}$ was observed while the association of $Isw1_{\Delta SANT}$ and $Isw1_{\Delta SLIDE}$ to chromatin was reduced three- to fivefold, similar to that observed with *MET16*. Similarly, at *FMP27* and the chromosome V intergenic region, low levels of WT Isw1 and $Isw1_{K227R}$ are evident but the levels are significantly lower in the strains expressing $Isw1_{\Delta SANT}$ and $Isw1_{\Delta SLIDE}$. This suggests that $Isw1_{\Delta SANT}$ and $Isw1_{\Delta SLIDE}$ do not show relaxed specificity but a reduced capacity to maintain their interaction with chromatin. Thus, the SANT and SLIDE domains are likely to influence Isw1 association with chromatin.

Upon activation of *MET16*, levels of Isw1 association with chromatin decrease up to 50% at the promoter (Fig. 4B). Nucleosome loss and histone H4 acetylation are observed at the active *MET16* gene, particularly at the promoter (44), and these changes to the nucleosomal substrate could account in part for the reduced Isw1 association with the active gene. Deletion of either the SANT or the SLIDE domain results in up to a fivefold drop of Isw1 occupancy at the *MET16* locus, though the signal remains higher than in the strain expressing $Isw1_{\Delta c}$. We considered a number of possibilities. SANT and SLIDE may stabilize direct interactions with histones and/or DNA. Alternatively, the reduced capacity of $Isw1_{\Delta SANT}$ and $Isw1_{\Delta SLIDE}$ to interact with chromatin may be influenced by

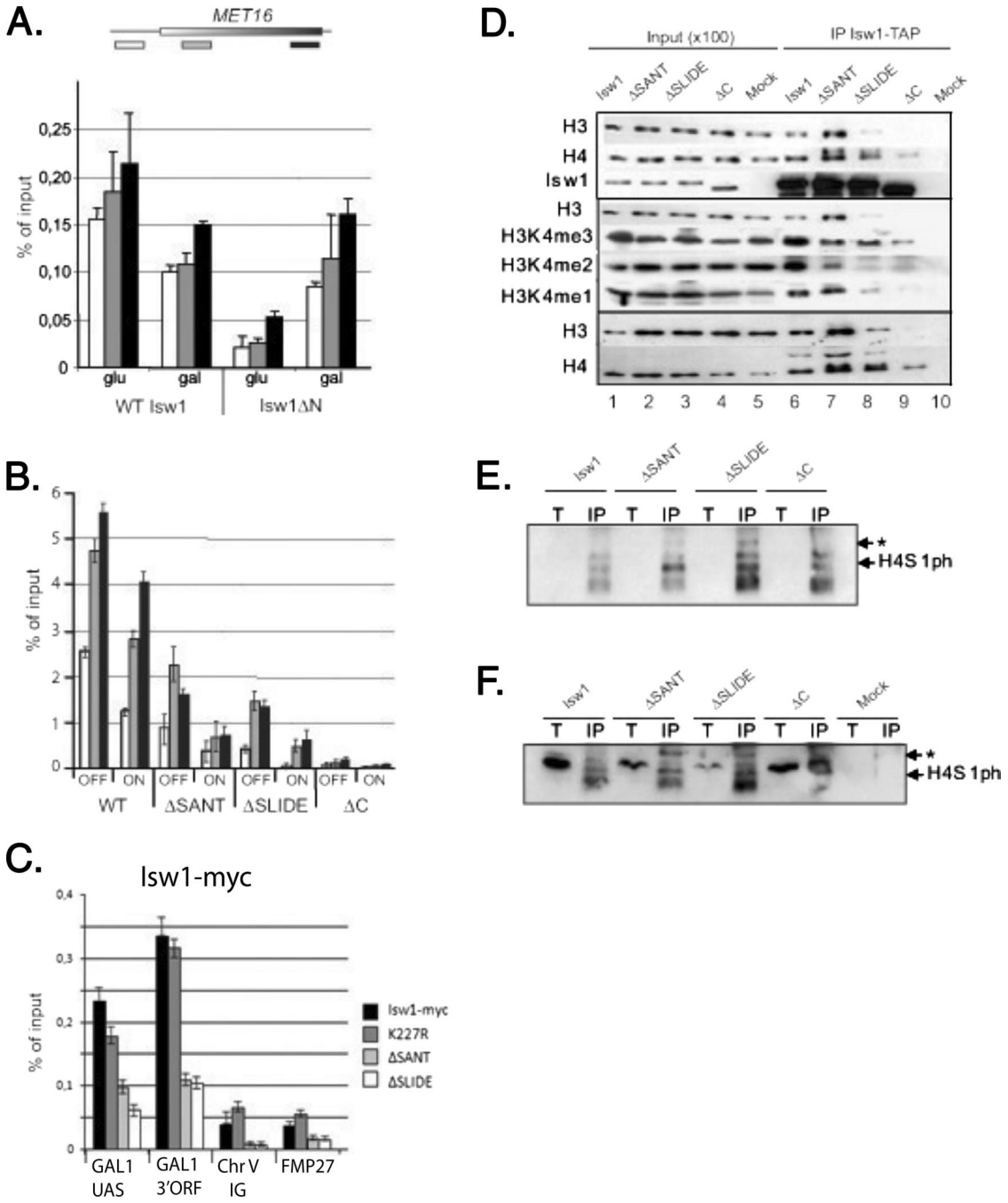

FIG. 4. The SANT and SLIDE domains are required for optimal Isw1 recruitment to chromatin and interactions with the nucleosomal substrate. (A) ChIP of TAP-tagged WT Isw1 and Isw1$_{\Delta N}$ across *MET16*. Isw1$_{\Delta N}$ expression is induced from the *GAL1* promoter. TAP-tagged WT Isw1 is grown under identical conditions. (B and C) ChIP of Myc-tagged Isw1 (WT) and deletion derivatives to the *MET16* locus under repressed conditions (OFF) and upon activation (ON) (B) or the induced *GAL* locus, *FMP27*, or an intergenic region on chromosome V (Chr V IG) (C). (D) Coimmunoprecipitation (IP) of TAP-tagged Isw1 and derivatives, with histones H3 and H4 subjected to the posttranslational modifications shown. The input sample (0.01%) is shown. (E and F) Coimmunoprecipitation of TAP-tagged Isw1 and derivatives, with histone H4 subject to phosphorylation at serine 1 (H4S1ph) (E) or both H4S1ph and H2BS1ph (F). Only H2BS1ph is evident in the total input material (T). A species migrating at 17 kDa is shown by an asterisk. The input sample (0.01%) is shown (T). glu, glucose; gal, galactose.

Isw1-associated proteins or result from changes to the chromatin template.

Distinct roles for the SANT and SLIDE domains in interactions with histone proteins. To explore whether the reduced association of Isw1$_{\Delta SANT}$ and Isw1$_{\Delta SLIDE}$ with chromatin results from a change in their interactions with histone proteins, we immunoprecipitated TAP-tagged Isw1 proteins and tested them for the presence of histones H3 and H4 in protein pull-down assays by Western blotting (Fig. 4D). WT Isw1 copurifies with both histone H3 and histone H4 (Fig. 4D, lane 6). As yeast

Isw1 associates indirectly but specifically with a histone H3 peptide when either dimethylated or trimethylated (52), we examined the modification state of histone H3 in the pull-down assay with Isw1. All three modifications are evident on histone H3 in the pull-down assay, with particular enrichment for H3K4me2 and H3K4me3 compared to the input material.

We found that Isw1$_{\Delta SANT}$ also copurifies with histones H3 and H4 (Fig. 4D, lane 7), suggesting that the SANT domain of Isw1 is not required for H3-H4 interactions. In fact, we observed that Isw1$_{\Delta SANT}$ reproducibly associated with more histones H3 and H4 than the WT strain, suggesting that Isw1$_{\Delta SANT}$ shows a higher affinity for these histones than the WT strain, perhaps as a result of altered posttranslational modifications. In support of this, Isw1$_{\Delta SANT}$ is associated with distinctly different modified histones. We reproducibly observed a change in the H3 methylation profile, with selection against dimethylated lysine 4, and an additional form of H4, with shifted migration on the gel, in the Isw1$_{\Delta SANT}$ pull-down assay (Fig. 4D, lane 7). Using an antibody specific to H4S1ph (Abcam) (Fig. 4E) or to both H4S1ph and H2BS1ph (Millipore) (Fig. 4F), we show that H4 phosphorylated at S1 is likely to be specifically associated with Isw1$_{\Delta SANT}$. There appears to be no detectable H4S1ph in the total extracts, consistent with previous observations that this is not an abundant modification in total chromatin. There is, however, a strong band at the position expected for H2BS1ph in the input material when the Millipore antibody is used. We note that a band migrating at about 17 kDa also shows a specific signal with these antibodies, but its identity is not clear. Phosphorylation often induces a mobility shift on gels, and histone H4 is known to be phosphorylated on serine 1 during DNA damage (7) and transcription (58). Specifically, serine 1 phosphorylation is associated with a reduced activity of the NuA4 HAT and loss of H4 acetylation (58). H4 acetylation strongly inhibits substrate recognition by DmISWI in vitro and in vivo (9, 11), raising the interesting possibility that nucleosome remodeling by yeast Isw1 might also require H4S1ph and associated deacetylation of H4 and that Isw1$_{\Delta SANT}$ captures an intermediate in the process.

Next, we examine the histone profile in the immunoprecipitates from the strain expressing Isw1$_{\Delta SLIDE}$. In contrast to Isw1$_{\Delta SANT}$, there is a significant reduction in the total amount of H3 and, to a lesser extent, H4 in the Isw1$_{\Delta SLIDE}$ pull-down assay (Fig. 4D, lane 8). We note that although there is very little histone H3 in the Isw1$_{\Delta SLIDE}$ pull-down assay compared to that in the WT assay, this appears to be specifically enriched for K4me3 but not H3K4me2. In addition, the H4 phosphorylated at S1 is also evident in the population of H4 molecules. The enrichment for H4 over H3 in the Isw1$_{\Delta SLIDE}$ pull-down assay is surprising since H3/H4 are usually considered to be in a complex within the nucleosomes or as free histones in association with chaperones. Loss of the SANT and SLIDE domains within the C-terminal region of Isw1 (Isw1$_{\Delta C}$) results in a very low signal for histone H3 (trimethylated at K4) and a significant reduction in H4 association.

These data suggest that the SANT motif is dispensable for the interaction between Isw1 and H3/H4. However, loss of the SANT domain leads to Isw1 associating with histones carrying a profile of modifications different from that carried by WT Isw1. For example, the interaction with chromatin modified with H4S1ph may reflect intermediates in Isw1 functions on chromatin while the changes in the H3K4 methylation profiles might reflect the stability of the interactions. In addition, the association of Isw1 with chromatin may not solely reflect histone binding. There may also be interactions with DNA, a function most likely to be associated with the positively charged SANT domain. We cannot, however, rule out the possibility that other proteins play a role in tethering Isw1 to chromatin via the SANT and SLIDE domains. Possible candidates are the Ioc proteins, components of Isw1 complexes in vivo.

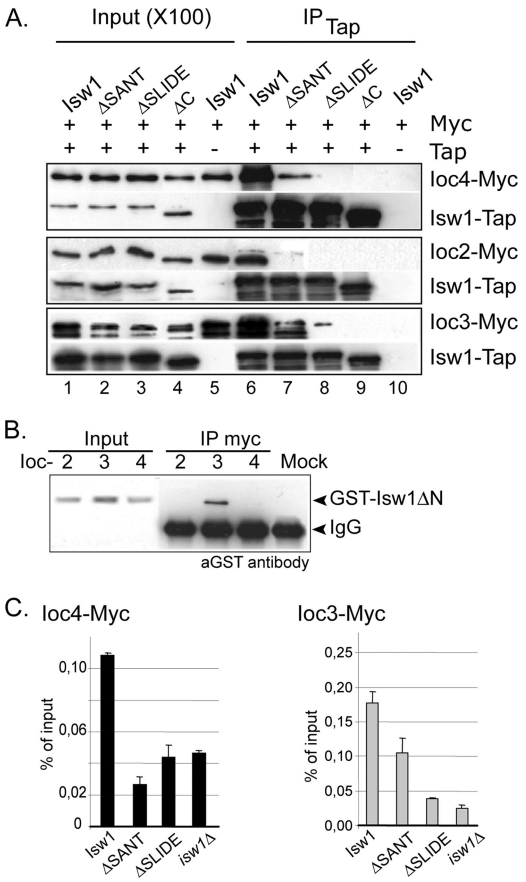

FIG. 5. SANT and SLIDE are required differentially for interaction with Ioc proteins. (A) Coimmunoprecipitation (IP) of Myc-tagged Ioc proteins with TAP-tagged Isw1 WT and deletion derivatives. (B) Coimmunoprecipitation of Myc-tagged Ioc proteins with GST-tagged Isw1$_{\Delta N}$. (C) ChIP of Ioc4-Myc to the *MET16* 3′ ORF and Ioc3-Myc to the *MET16* promoter. IgG, immunoglobulin G.

The SANT and SLIDE domains interact with Ioc2 and Ioc4. To address whether the SANT or SLIDE domain of Isw1 interacts with Ioc proteins, we immunoprecipitated TAP-tagged Isw1 derivatives and tested them for the presence of Myc-tagged Ioc proteins in pull-down assays (Fig. 5). We found that the deletion of SLIDE resulted in a loss of Ioc2 and Ioc4 proteins in the immunoprecipitate (Fig. 5A, compare lanes 6 and 8). As expected, the same result was obtained in the case of Isw1$_{\Delta C}$, lacking the whole C-terminal part and localized to the cytoplasm (Fig. 5A, lane 9). Additionally, the association of Isw1 with Ioc2 and Ioc4 is significantly impaired when the SANT domain is deleted. It was previously shown that Ioc2

and Ioc4 are interdependent in their interaction with Isw1, as loss of either one results in the loss of the other during the purification of the Isw1b complex (59). It is not known whether they both interact with Isw1 or whether the binding is mediated by one of the pair. However, our results demonstrate that the association of the Ioc2p/Ioc4p heterodimer with Isw1 needs the integrity of the C-terminal region, including both the SANT and SLIDE domains.

To address whether the C-terminal region of Isw1 containing the SANT and SLIDE domains is sufficient for interactions with Ioc2 and Ioc4 proteins, we immunoprecipitated Myc-tagged Ioc proteins in the strain expressing 386 glutathione *S*-transferase (GST)-tagged C-terminal amino acids of Isw1 ($Isw1_{\Delta N}$) and tested them for the presence of $Isw1_{\Delta N}$ in pull-down assays (Fig. 5B). No interaction is observed with either Ioc2 or Ioc4. This suggests that the interaction between Isw1, Ioc2, and Ioc4 requires more than sequences in the 386 C-terminal amino acids of Isw1.

Finally, to confirm the results of coimmunoprecipitation, we performed ChIP of Myc-tagged Ioc4 in the *isw1*Δ strain and strains expressing $Isw1_{\Delta SANT}$ and $Isw1_{\Delta SLIDE}$ under inducing growth conditions (Fig. 5C). We found that Ioc4 recruitment to *MET16* is strongly diminished in strains expressing $Isw1_{\Delta SANT}$ and $Isw1_{\Delta SLIDE}$. Interestingly, we note that Ioc4 gives a significant signal at the *MET16* locus even in the absence of Isw1, suggesting that Ioc4 may also interact with chromatin independently of Isw1 and the Isw1b complex.

The SLIDE domain, but not the SANT domain, is required for an interaction with Ioc3. To address whether the C-terminal region of Isw1 is sufficient for interactions with Ioc3, we immunoprecipitated Myc-tagged Ioc3 and tested it for the presence of 386 GST-tagged C-terminal amino acids of Isw1 in the pull-down assay (Fig. 5B). A clear interaction of Ioc3 with the C-terminal region of Isw1 is observed.

Then, we examined the regions of Isw1 required for interaction with Ioc3 (Fig. 5A, bottom panel). Interestingly, in the strain expressing $Isw1_{\Delta SANT}$, significant amounts of Ioc3 are present in the coimmunoprecipitate. A much weaker interaction is observed in the strain expressing $Isw1_{\Delta SLIDE}$, supporting a role for the SLIDE domain in Ioc3 binding.

From previous work, we knew that Ioc3, as a part of the Isw1a complex, is recruited to *MET16*, assisting Isw1 in a specific promoter-proximal dinucleosome positioning and repression of transcription initiation (45). Thus, the next question we addressed is whether Ioc3 is recruited to the *MET16* locus in the presence of Isw1 lacking the SANT or SLIDE domain (Fig. 5C). In the absence of Isw1, Ioc3 levels at the *MET16* locus are significantly reduced, suggesting that Ioc3 recruitment to this locus is in part Isw1 dependent. Deletion of the SLIDE domain also causes a loss of Ioc3 association with chromatin, similar to that when Isw1 is absent. In contrast, loss of the SANT domain resulted in a modest reduction in Ioc3 association with chromatin. Furthermore, given that levels of Isw1 association itself are reduced by this amount in the absence of the SANT domain (Fig. 4B), we conclude first that the SANT domain is unlikely to play a major role in Ioc3 association with Isw1 or with chromatin and second that the SLIDE domain is important for Ioc3 tethering to *MET16*. These observations led us to ask whether the presence of $Isw1_{\Delta SANT}$ and Ioc3 at the *MET16* locus influences chromatin remodeling or transcription.

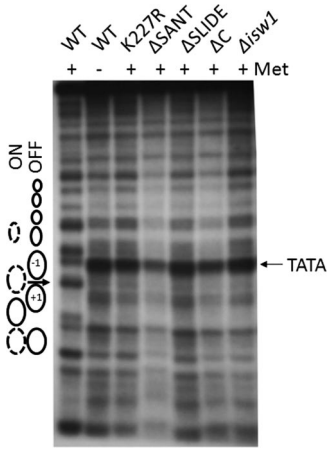

FIG. 6. Isw1 lacking the SANT or SLIDE domain fails to remodel nucleosomes at the *MET16* locus in vivo. Indirect end label analysis of MNase-cleaved and EcoRI-restricted chromatin prepared from the indicated strains cultured in the presence (OFF) or absence (ON) of methionine. The previously mapped nucleosomes (44, 45) (−1 over the TATA box and +1 spanning the beginning of the ORF) and the changes that occur upon activation are shown on the schematic. The hypersensitive site (thick arrow) flanked by nucleosomes −1 and +1 is lost upon activation and is accompanied by the generation of a hypersensitive region around the TATA box (TATA arrow). The probe abuts the EcoRI site within the *MET16* ORF.

Chromatin remodeling in vivo is defective in strains expressing $Isw1_{\Delta SANT}$ and $Isw1_{\Delta SLIDE}$. Under repressive conditions, Isw1 shifts two nucleosomes (−1 and +1) over the *MET16* promoter, masking a TATA box (44, 45). Upon activation or in the absence of Isw1, the promoter adopts an open structure and becomes more accessible to the transcription machinery, allowing more-efficient transcription initiation. Isw1 controls the rate of these changes (44). To determine whether SANT and SLIDE contribute to the remodeling activity of Isw1, we performed MNase mapping of chromatin at the *MET16* locus. Under repressive conditions, there is a hypersensitive site between nucleosomes −1 and +1 at the *MET16* locus (Fig. 6, lane 1). If Isw1 is absent or catalytically inactive (Fig. 6, lanes 3 and 7), the cleavage pattern at the repressed promoter resembles that of the WT promoter when induced (Fig. 6, lane 2) (45). In strains expressing $Isw1_{\Delta SANT}$ and $Isw1_{\Delta SLIDE}$, the nucleosome positioning patterns are similar and resemble those of $Isw1_{K227R}$ and the *isw1*Δ strain or the WT activated by starvation for methionine. Thus, the deletion of either SANT or SLIDE abolishes the nucleosome remodeling activity of Isw1. This failure to remodel nucleosomes may result simply from the reduced association of $Isw1_{\Delta SANT}$ and $Isw1_{\Delta SLIDE}$ with chromatin, a change in the off rate for the enzyme/chromatin complex, or the loss of a key anchoring interaction, such as that involving DNA, histones, or Isw1-interacting proteins. At present, we are unable to separate these. Due to problems obtaining full-length Isw1 protein in *Escherichia coli*, we were unable to ask whether the SANT and SLIDE domains are absolutely required for ATPase activity and nucleosome remodeling by Isw1 or whether they provide anchoring sites for the Ioc proteins which determine

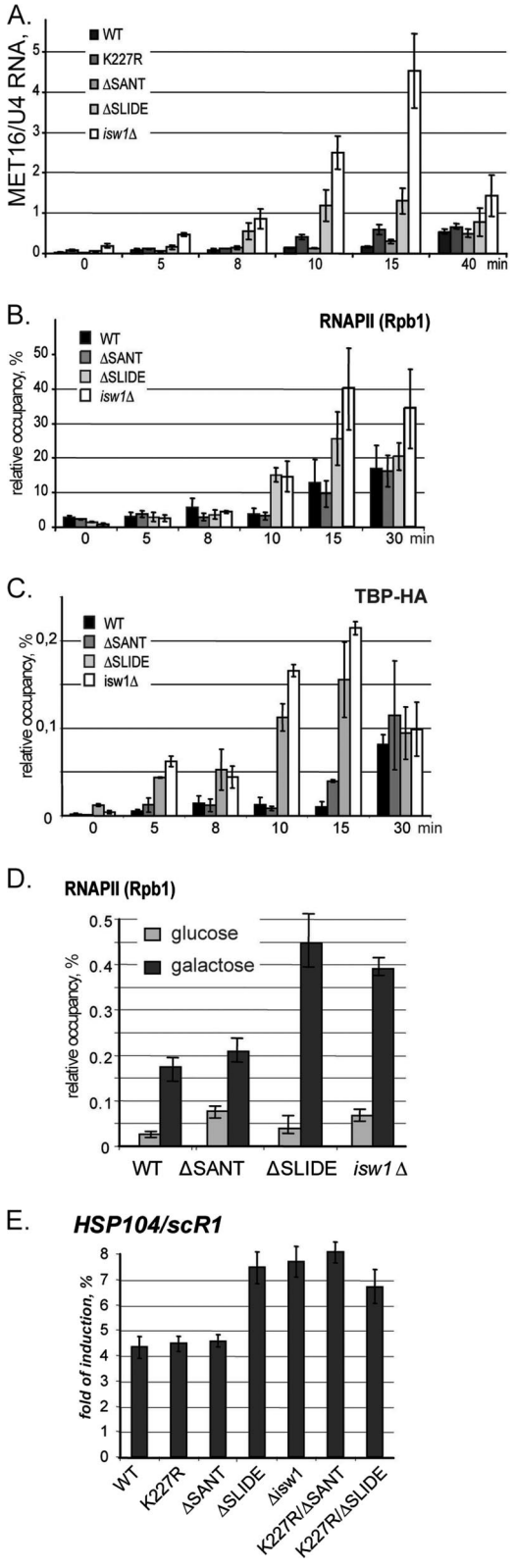

FIG. 7. SLIDE, but not SANT, controls the timing of *MET16* transcription initiation, causing a delay in TBP and RNAPII recruitment to the promoter region upon activation. (A) *MET16* RNA abundance, quantified by reverse-transcribed real-time PCR. U4 snRNA was used as a reference, and the signal is expressed as a ratio of *MET16* RNA/U4. (B) Association of RNAPII (Rpb1) with the *MET16* 5′ ORF in strains expressing full-length Isw1 and deletion derivatives and strains lacking Isw1. ChIP signals were normalized to that of tF(GAA)P2. (C) Association of TBP with the *MET16* promoter in strains expressing full-length Isw1 and deletion derivatives and strains lacking Isw1. ChIP signals were normalized to that of tF(GAA)P2. (D) Levels of RNAPII at the 3′ region of the *GAL1* ORF in the strains shown from cells grown in glucose or induced for 60 min in galactose. The high residual levels of RNAPII in the strains lacking functional Isw1 are due to a long regulatory transcript normally repressed by an Isw1-positioned nucleosome. ChIP signals were normalized to that of tF(GAA)P2. (E) Levels of *HSP104* transcript, normalized to scR1 and shown relative to that of the uninduced signal, for two samples subjected to heat shock for 10 min in the strain backgrounds shown.

the outcome of the remodeling reaction (55). Further work in vitro will be required to fully assess the role of the SANT and SLIDE domains in the ATPase and remodeling activities of Isw1 in vitro.

The SLIDE domain provides transcriptional repression at the *MET16* locus. According to the existing models, Isw1, as a part of the Isw1a complex, represses initiation of transcription of *MET16* (45). After withdrawal of methionine from the medium, the *MET16* transcript appears between 5 and 10 min, reaching maximal levels between 20 and 40 min, although the precise timing depends on the strain background used. In the Isw1-depleted strain, the *MET16* transcript is evident in the repressed culture and rapidly peaks to above maximal levels observed in the WT strain (Fig. 7A) (45). To explore whether the SLIDE and SANT domains play a role in the repression of transcription initiation at the *MET16* locus, we assess the time at which the *MET16* mRNA appears upon induction by quantitative reverse transcription-PCR (Fig. 7A) and Northern blotting (data not shown).

In this experiment, the absence of Isw1 leads to a failure to fully repress *MET16* and more-abundant transcript levels in derepressed cultures. Significantly, the strain expressing the catalytically inactive Isw1 mutant, $Isw1_{K227R}$, shows an intermediate profile between the WT and *isw1*Δ strains, suggesting that a defect in chromatin remodeling is not the only explanation for transcription repression by Isw1. The transcription profile of $Isw1_{\Delta SANT}$ is the same as that of the WT, suggesting that the SANT domain plays no role in transcriptional repression at the *MET16* locus. In contrast, the profile for the strain expressing $Isw1_{\Delta SLIDE}$ is intermediate between $Isw1_{K227R}$ and the *isw1*Δ strain. This result suggests that the C-terminal part of Isw1 lacking the SANT domain can produce retardation of *MET16* mRNA transcription in the absence of the ATP-dependent nucleosome remodeling activity of Isw1.

Transcription is a complex process with several successive steps, including activation and RNAPII recruitment, transcription initiation, elongation, termination, and RNA processing. Defects in each step can have an impact on final mRNA levels. To further define a role for the C-terminal domain in repression of transcription, we performed a ChIP experiment to examine the time at which RNAPII and TBP become detectable at the 5′ ORF (Fig. 7B) and *MET16* promoter (Fig. 7C), respectively, upon induction. Strains expressing $Isw1_{\Delta SANT}$ and $Isw1_{\Delta SLIDE}$ were compared to the *isw1*Δ strain. We found that the deletion of SLIDE, as well as the absence of Isw1, resulted

in earlier recruitment of RNAPII to the coding region of the gene (Fig. 7B, 10-min time point). The strain expressing Isw1$_{\Delta SANT}$ behaved like the WT, with a 5-min delay before RNAPII was observed on the ORF, compared to the strain expressing Isw1$_{\Delta SLIDE}$. TBP appearance at the *MET16* promoter showed the same differences between strains expressing Isw1$_{\Delta SANT}$ and Isw1$_{\Delta SLIDE}$. In the strain expressing Isw1$_{\Delta SLIDE}$, TBP appears 10 min earlier than in the WT and the strain expressing Isw1$_{\Delta SANT}$. To see whether these functions are evident in other genes, we examined RNAPII or RNA levels at two additional regulated loci, those of *GAL1* and *HSP104*. Sixty minutes after induction, levels of RNAPII at the 3′ region of *GAL1* are significantly higher in Isw1$_{\Delta SLIDE}$ and the *isw1*Δ strain than in Isw1$_{\Delta SANT}$ or the WT (Fig. 7D). Similarly, at the *HSP104* locus, transcript levels follow the same general pattern as that observed at the *MET16* or *GAL1* locus after a 10-min heat shock (Fig. 7E). Moreover, unlike the WT, strains lacking both ATPase activity and the SANT domain fail to repress, supporting a redundant function for Isw1 in repressing early-onset transcription initiation. We conclude that the SLIDE domain plays a role in transcriptional repression in a mechanism that is likely to be independent of the ATPase activity of Isw1.

DISCUSSION

Isw1 functions in transcription regulation and chromatin remodeling in vivo. There are strong correlations between the nucleosome remodeling activity of Isw1 and transcriptional repression (12, 45, 53), and current models link these two functions although direct evidence is lacking. Moreover, information concerning the structural and biochemical aspects of the SANT and SLIDE domains supports their involvement in nucleosome mobilization and reorganization (13, 21). We show here that the Isw1 SANT and SLIDE domains are required for nucleosome positioning at the *MET16* promoter in vivo, but whether this relates to a direct effect of the SANT/SLIDE domains on ATPase activity or simply defects in the recruitment of sufficient amounts of Isw1 is not clear at present. Whatever the explanation for the failure of Isw1$_{\Delta SANT}$ and Isw1$_{\Delta SLIDE}$ to remodel nucleosomes, we show that transcriptional repression occurs normally in Isw1$_{\Delta SANT}$. Moreover, Isw1$_{\Delta SANT}$ is able to form an interaction with Ioc3, supporting a role for the Isw1a complex in transcriptional repression. Thus, this work provides an example of transcriptional control by a chromatin-remodeling ATPase that is independent of its nucleosome remodeling activity.

In the fly and *Xenopus laevis* ISWI, the negatively charged SANT domain is proposed to be involved in histone interactions (21, 26) while the positively charged SLIDE domain is likely to interact with DNA (21), combining to facilitate protein binding to the nucleosomal substrate. The yeast Isw2 ATPase scaffold, formed in a part by SANT and SLIDE, has been shown to establish contacts with DNA in the entry/exit site of the nucleosome, providing unidirectional movement of the DNA (13). In yeast Isw1, the two closely spaced SANT motifs show high homology to fly ISWI and yeast Isw2 domains, although in Isw1 they differ in surface charge distributions and associated functions. Thus, in Isw1, the SLIDE domain interacts with histones while the fly and Isw2 SLIDE domains interact with DNA. The different charge distributions in the SANT and SLIDE domains between Isw1 and Isw2 are unlikely to reflect differences in remodeling activity per se since, in vitro, Isw1a and Isw2 show similar specificities which differ from that of Isw1b (55). However, these differences may reflect protein-protein interactions (with Itc1 or the Ioc proteins, for example) or covalent modifications to the substrate in vivo which require different charge distributions. The possibility that ISWI-like enzymes function as dimers suggests interactions with both the substrate and the enzyme and may include other functional components such as Ioc proteins (50), known to stimulate ATPase activity in vitro (59). Thus, while functioning as ATPases, there may be redundancy in the mechanism used to mediate substrate and enzyme interactions within this family.

Strains expressing Isw1$_{\Delta SANT}$ lack the Isw1b (Isw1, Ioc2, and Ioc4) complex but have a form of the Isw1a (Isw1 and Ioc3) complex that is not able to remodel nucleosomes in vivo. Our data suggest that this form of Isw1a is sufficient to mediate transcriptional repression at the *MET16* locus. This is entirely consistent with previous data showing that Ioc3 influences repression at the *MET16* locus (45) and other loci (12), often acting redundantly with factors such as Esc8 and Esc2. Taking into account that neither Isw1$_{\Delta SANT}$ nor Isw1$_{\Delta SLIDE}$ is competent to remodel nucleosomes, it is likely that Isw1$_{\Delta SANT}$ affects transcription via protein-protein interactions, thus playing a scaffold function. A candidate for Isw1/Ioc3-mediated repression is TAF1, a component of TFIID, known to have both activatory and inhibitory effects on transcription (10, 23, 51). Isw1/Ioc3 is found in complexes with Mot1, an enzyme that displaces TBP from DNA (2), perhaps explaining its influence on the timing of TBP association at the *MET16* locus (19). Isw1/Ioc3 is also a component of the Sin3 deacetylation complex (19, 20) together with components of the NuA4 acetyltransferase and casein kinase. Deacetylation of H4 represses transcription and is likely to be required for Isw1a-mediated nucleosome remodeling. Casein kinase phosphorylates H4 serine 1, leading to inhibition of NuA4 activity and promoting Sin3-dependent H4 deacetylation (58) and offering another explanation for Isw1a-mediated repression. This could lead to nucleosome remodeling, dephosphorylation of H4S1ph and subsequent histone acetylation, and fixing of the nucleosome position, perhaps also contributing to repression. The ability of the remodeling-deficient forms of Isw1 to trap H4S1ph could represent an intermediate in this series of events.

This work suggests that Isw1 has roles as both an ATPase and a scaffold supporting protein-protein interactions, both of which play roles in Isw1-mediated repression of transcription. We have already described protein-protein interactions requiring the integrity of Isw1, but not its ATPase activity, that mediate Isw2-dependent nucleosome sliding and transcriptional repression at the *CLB2* promoter (53). Just as observed at the *MET16* locus, Isw1 remodels a limited region at the *CLB2* locus, comprising two nucleosomes linking the promoter to the beginning of the ORF. However, the data presented here suggest that protein-protein interactions may be as important as ATPase activity for Isw1 repressive function in vivo. TAP tag pull-down assay data and synthetic genetic interactions indicate that Isw1 interacts with proteins involved not

only in transcription but also in DNA replication and repair. It remains to be seen how the C-terminal domain of Isw1 including the SANT and SLIDE domains functions in these processes.

ACKNOWLEDGMENTS

This work was supported by a FEBS fellowship to M.P., ATIPE (CNRS) and HFSPO to A.M., and the Wellcome Trust (J.M.).

We thank Laurant Kuras for the plasmid expressing HA-tagged TBP and Toshio Tsukiyama for the strain expressing $Isw1_{K227R}$.

REFERENCES

1. **Aasland, R., A. F. Stewart, and T. Gibson.** 1996. The SANT domain: a putative DNA-binding domain in the SWI-SNF and ADA complexes, the transcriptional co-repressor N-coR and TFIIB. Trends Biochem. Sci. **21:** 87–88.
2. **Auble, D., K. Hansen, C. Mueller, W. Lane, J. Thorner, and S. Hahn.** 1994. Mot1, a global repressor of RNA polymerase II transcription, inhibits TBP binding to DNA by an ATP-dependent mechanism. Genes Dev. **8:**1920–1934.
3. **Baudin, A., O. Ozier-Kalogeropoulos, A. Denouel, F. Lacroute, and C. Cullin.** 1993. A simple and efficient method for direct gene deletion in Saccharomyces cerevisiae. Nucleic Acids Res. **21:**3329–3330.
4. **Boyer, L. A., M. R. Langer, K. A. Crowley, S. Tan, J. M. Denu, and C. L. Peterson.** 2002. Essential role for the SANT domain in the functioning of multiple chromatin remodeling enzymes. Mol. Cell **10:**935–942.
5. **Boyer, L. A., R. R. Latek, and C. L. Peterson.** 2004. The SANT domain: a unique histone-tail-binding module? Nat. Rev. Mol. Cell Biol. **5:**158–163.
6. **Burke, D. J., D. Dawson, and T. Stearns.** 2000. Methods in yeast genetics: a Cold Spring Harbor Laboratory course manual, p. 133–135. Cold Spring Harbor Laboratory Press, Cold Spring Harbor, NY.
7. **Cheung, W. L., F. B. Turner, T. Krishnamoorthy, B. Wolner, S. H. Ahn, M. Foley, J. A. Dorsey, C. L. Peterson, S. L. Berger, and C. D. Allis.** 2005. Phosphorylation of histone H4 serine 1 during DNA damage requires casein kinase II in S. cerevisiae. Curr. Biol. **15:**656–660.
8. **Clapier, C. R., G. Langst, D. F. Corona, P. B. Becker, and K. P. Nightingale.** 2001. Critical role for the histone H4 N terminus in nucleosome remodeling by ISWI. Mol. Cell. Biol. **21:**875–883.
9. **Clapier, C. R., K. P. Nightingale, and P. B. Becker.** 2002. A critical epitope for substrate recognition by the nucleosome remodeling ATPase ISWI. Nucleic Acids Res. **30:**649–655.
10. **Collins, S. R., K. M. Miller, N. L. Maas, A. Roguev, J. Fillingham, C. S. Chu, M. Schuldiner, M. Gebbia, J. Recht, M. Shales, H. Ding, H. Xu, J. Han, K. Ingvarsdottir, B. Cheng, B. Andrews, C. Boone, S. L. Berger, P. Hieter, Z. Zhang, G. W. Brown, C. J. Ingles, A. Emili, C. D. Allis, D. P. Toczyski, J. S. Weissman, J. F. Greenblatt, and N. J. Krogan.** 2007. Functional dissection of protein complexes involved in yeast chromosome biology using a genetic interaction map. Nature **446:**806–810.
11. **Corona, D. F., C. R. Clapier, P. B. Becker, and J. W. Tamkun.** 2002. Modulation of ISWI function by site-specific histone acetylation. EMBO Rep. **3:**242–247.
12. **Cuperus, G., and D. Shore.** 2002. Restoration of silencing in Saccharomyces cerevisiae by tethering of a novel Sir2-interacting protein, Esc8. Genetics **162:**633–645.
13. **Dang, W., and B. Bartholomew.** 2007. Domain architecture of the catalytic subunit in the ISW2-nucleosome complex. Mol. Cell. Biol. **27:**8306–8317.
14. **Dang, W., M. N. Kagalwala, and B. Bartholomew.** 2006. Regulation of ISW2 by concerted action of histone H4 tail and extranucleosomal DNA. Mol. Cell. Biol. **26:**7388–7396.
15. **Ding, Z., L. L. Gillespie, F. C. Mercer, and G. D. Paterno.** 2004. The SANT domain of human MI-ER1 interacts with Sp1 to interfere with GC box recognition and repress transcription from its own promoter. J. Biol. Chem. **279:**28009–28016.
16. **Ebralidse, K. K., S. A. Grachev, and A. D. Mirzabekov.** 1988. A highly basic histone H4 domain bound to the sharply bent region of nucleosomal DNA. Nature **331:**365–367.
17. **Flanagan, J. F., L. Z. Mi, M. Chruszcz, M. Cymborowski, K. L. Clines, Y. Kim, W. Minor, F. Rastinejad, and S. Khorasanizadeh.** 2005. Double chromodomains cooperate to recognize the methylated histone H3 tail. Nature **438:**1181–1185.
18. **Gangaraju, V. K., and B. Bartholomew.** 2007. Dependency of ISW1a chromatin remodeling on extranucleosomal DNA. Mol. Cell. Biol. **27:**3217–3225.
19. **Gavin, A. C., P. Aloy, P. Grandi, R. Krause, M. Boesche, M. Marzioch, C. Rau, L. J. Jensen, S. Bastuck, B. Dumpelfeld, A. Edelmann, M. A. Heurtier, V. Hoffman, C. Hoefert, K. Klein, M. Hudak, A. M. Michon, M. Schelder, M. Schirle, M. Remor, T. Rudi, S. Hooper, A. Bauer, T. Bouwmeester, G. Casari, G. Drewes, G. Neubauer, J. M. Rick, B. Kuster, P. Bork, R. B. Russell, and G. Superti-Furga.** 2006. Proteome survey reveals modularity of the yeast cell machinery. Nature **440:**631–636.
20. **Gavin, A. C., M. Bosche, R. Krause, P. Grandi, M. Marzioch, A. Bauer, J. Schultz, et al.** 2002. Functional organization of the yeast proteome by systematic analysis of protein complexes. Nature **415:**141–147.
21. **Grune, T., J. Brzeski, A. Eberharter, C. R. Clapier, D. F. V. Corona, P. B. Becker, and C. W. Muller.** 2003. Crystal structure and functional analysis of a nucleosome recognition module of the remodeling factor ISWI. Mol. Cell **12:**449–460.
22. **Guenther, M. G., O. Barak, and M. A. Lazar.** 2001. The SMRT and N-CoR corepressors are activating cofactors for histone deacetylase 3. Mol. Cell. Biol. **21:**6091–6101.
23. **Guermah, M., Y. Tao, and R. G. Roeder.** 2001. Positive and negative TAF_{II} functions that suggest a dynamic TFIID structure and elicit synergy with TRAPs in activator-induced transcription. Mol. Cell. Biol. **21:**6882–6894.
24. **Hassan, A. H., S. Awad, Z. Al-Natour, S. Othman, F. Mustafa, and T. A. Rizvi.** 2007. Selective recognition of acetylated histones by bromodomains in transcriptional co-activators. Biochem. J. **402:**125–133.
25. **Hassan, A. H., P. Prochasson, K. E. Neely, S. C. Galasinski, M. Chandy, M. J. Carrozza, and J. L. Workman.** 2002. Function and selectivity of bromodomains in anchoring chromatin-modifying complexes to promoter nucleosomes. Cell **111:**369–379.
26. **Horton, J. R., S. J. Elgar, S. I. Khan, X. Zhang, P. A. Wade, and X. Cheng.** 2007. Structure of the SANT domain from the Xenopus chromatin remodeling factor ISWI. Proteins **67:**1198–1202.
27. **Huang, Y., J. Fang, M. T. Bedford, Y. Zhang, and R. M. Xu.** 2006. Recognition of histone H3 lysine-4 methylation by the double tudor domain of JMJD2A. Science **312:**748–751.
28. **Hughes, R. M., K. R. Wiggins, S. Khorasanizadeh, and M. L. Waters.** 2007. Recognition of trimethyllysine by a chromodomain is not driven by the hydrophobic effect. Proc. Natl. Acad. Sci. USA **104:**11184–11188.
29. **Iyer, V., and K. Struhl.** 1996. Absolute mRNA levels and transcriptional initiation rates in Saccharomyces cerevisiae. Proc. Natl. Acad. Sci. USA **93:**5208–5212.
30. **Kent, N. A., L. E. Bird, and J. Mellor.** 1993. Chromatin analysis in yeast using NP-40 permeabilised sphaeroplasts. Nucleic Acids Res. **21:**4653–4654.
31. **Kent, N. A., N. Karabetsou, P. K. Politis, and J. Mellor.** 2001. In vivo chromatin remodeling by yeast ISWI homologs Isw1p and Isw2p. Genes Dev. **15:**619–626.
32. **Kim, Y., N. McLaughlin, K. Lindstrom, T. Tsukiyama, and D. J. Clark.** 2006. Activation of *Saccharomyces cerevisiae HIS3* results in Gcn4p-dependent, SWI/SNF-dependent mobilization of nucleosomes over the entire gene. Mol. Cell. Biol. **26:**8607–8622.
33. **Kuras, L., T. Borggrefe, and R. D. Kornberg.** 2003. Association of the Mediator complex with enhancers of active genes. Proc. Natl. Acad. Sci. USA **100:**13887–13891.
34. **Lan, F., R. E. Collins, R. De Cegli, R. Alpatov, J. R. Horton, X. Shi, O. Gozani, X. Cheng, and Y. Shi.** 2007. Recognition of unmethylated histone H3 lysine 4 links BHC80 to LSD1-mediated gene repression. Nature **448:** 718–722.
35. **Li, B., M. Gogol, M. Carey, D. Lee, C. Seidel, and J. L. Workman.** 2007. Combined action of PHD and chromo domains directs the Rpd3S HDAC to transcribed chromatin. Science **316:**1050–1054.
36. **Li, H., S. Ilin, W. Wang, E. M. Duncan, J. Wysocka, C. D. Allis, and D. J. Patel.** 2006. Molecular basis for site-specific read-out of histone H3K4me3 by the BPTF PHD finger of NURF. Nature **442:**91–95.
37. **Lindstrom, K. C., J. C. Vary, Jr., M. R. Parthun, J. Delrow, and T. Tsukiyama.** 2006. Isw1 functions in parallel with the NuA4 and Swr1 complexes in stress-induced gene repression. Mol. Cell. Biol. **26:**6117–6129.
38. **Longtine, M. S., A. McKenzie, D. J. Demarini, N. G. Shah, A. Wach, A. Brachat, P. Philippsen, and J. R. Pringle.** 1998. Additional modules for versatile and economical PCR-based gene deletion and modification in *Saccharomyces cerevisiae*. Yeast **14:**953–961.
39. **Mellor, J.** 2006. It takes a PHD to read the histone code. Cell **126:**22–24.
40. **Mellor, J., and A. Morillon.** 2004. ISWI complexes in Saccharomyces cerevisiae. Biochim. Biophys. Acta **1677:**100–112.
41. **Meluh, P. D., and J. R. Broach.** 1999. Immunological analysis of yeast chromatin. Methods Enzymol. **304:**414–430.
42. **Mo, X., E. Kowenz-Leutz, Y. Laumonnier, H. Xu, and A. Leutz.** 2005. Histone H3 tail positioning and acetylation by the c-Myb but not the v-Myb DNA-binding SANT domain. Genes Dev. **19:**2447–2457.
43. **Moreau, J.-L., M. Lee, N. Mahachi, J. C. Vary, Jr., J. Mellor, T. Tsukiyama, and C. Goding.** 2003. Regulated displacement of TBP from the *PHO8* promoter in vivo requires Cbf1 and the Isw1 chromatin remodeling complex. Mol. Cell **11:**1609–1620.
44. **Morillon, A., N. Karabetsou, A. Nair, and J. Mellor.** 2005. Dynamic lysine methylation on histone H3 defines the regulatory phase of gene transcription. Mol. Cell **18:**723–734.
45. **Morillon, A., N. Karabetsou, J. O'Sullivan, N. Kent, N. Proudfoot, and J. Mellor.** 2003. Isw1 chromatin remodeling ATPase coordinates transcription elongation and termination by RNA polymerase II. Cell **115:**425–435.
46. **Mueller, J. E., and M. Bryk.** 2007. Isw1 acts independently of the Isw1a and Isw1b complexes in regulating transcriptional silencing at the ribosomal DNA locus in Saccharomyces cerevisiae. J. Mol. Biol. **371:**1–10.

47. **Mujtaba, S., L. Zeng, and M. M. Zhou.** 2007. Structure and acetyl-lysine recognition of the bromodomain. Oncogene **26:**5521–5527.
48. **Ogata, K., S. Morikawa, H. Nakamura, A. Sekikawa, T. Inoue, H. Kanai, A. Sarai, S. Ishii, and Y. Nishimura.** 1994. Solution structure of a specific DNA complex of the Myb DNA-binding domain with cooperative recognition helices. Cell **79:**639–648.
49. **Pena, P. V., F. Davrazou, X. Shi, K. L. Walter, V. V. Verkhusha, O. Gozani, R. Zhao, and T. G. Kutateladze.** 2006. Molecular mechanism of histone H3K4me3 recognition by plant homeodomain of ING2. Nature **442:**31–32.
50. **Racki, L. R., and G. J. Narlikar.** 2008. ATP-dependent chromatin remodeling enzymes: two heads are not better, just different. Curr. Opin. Genet. Dev. **18:**137–144.
51. **Sanders, S. L., J. Jennings, A. Canutescu, A. J. Link, and P. A. Weil.** 2002. Proteomics of the eukaryotic transcription machinery: identification of proteins associated with components of yeast TFIID by multidimensional mass spectrometry. Mol. Cell. Biol. **22:**4723–4738.
52. **Santos-Rosa, H., R. Schneider, B. E. Bernstein, N. Karabetsou, A. Morillon, C. Weise, S. L. Schreiber, J. Mellor, and T. Kouzarides.** 2003. Methylation of histone H3 K4 mediates association of the Isw1p ATPase with chromatin. Mol. Cell **12:**1325–1332.
53. **Sherriff, J. A., N. A. Kent, and J. Mellor.** 2007. The Isw2 chromatin-remodeling ATPase cooperates with the Fkh2 transcription factor to repress transcription of the B-type cyclin gene *CLB2*. Mol. Cell. Biol. **27:**2848–2860.
54. **Sterner, D. E., X. Wang, M. H. Bloom, G. M. Simon, and S. L. Berger.** 2002. The SANT domain of Ada2 is required for normal acetylation of histones by the yeast SAGA complex. J. Biol. Chem. **277:**8178–8186.
55. **Stockdale, C., A. Flaus, H. Ferreira, and T. Owen-Hughes.** 2006. Analysis of nucleosome repositioning by yeast ISWI and Chd1 chromatin remodeling complexes. J. Biol. Chem. **281:**16279–16288.
56. **Taverna, S. D., H. Li, A. J. Ruthenburg, C. D. Allis, and D. J. Patel.** 2007. How chromatin-binding modules interpret histone modifications: lessons from professional pocket pickers. Nat. Struct. Mol. Biol. **14:**1025–1040.
57. **Tsukiyama, T., J. Palmer, C. C. Landel, J. Shiloach, and C. Wu.** 1999. Characterization of the imitation switch subfamily of ATP-dependent chromatin-remodeling factors in Saccharomyces cerevisiae. Genes Dev. **13:**686–697.
58. **Utley, R. T., N. Lacoste, O. Jobin-Robitaille, S. Allard, and J. Cote.** 2005. Regulation of NuA4 histone acetyltransferase activity in transcription and DNA repair by phosphorylation of histone H4. Mol. Cell. Biol. **25:**8179–8190.
59. **Vary, J. C., Jr., V. K. Gangaraju, J. Qin, C. C. Landel, C. Kooperberg, B. Bartholomew, and T. Tsukiyama.** 2003. Yeast Isw1p forms two separable complexes in vivo. Mol. Cell. Biol. **23:**80–91.
60. **Xella, B., C. Goding, E. Agricola, E. Di Mauro, and M. Caserta.** 2006. The ISWI and CHD1 chromatin remodelling activities influence ADH2 expression and chromatin organization. Mol. Microbiol. **59:**1531–1541.
61. **Yu, J., Y. Li, T. Ishizuka, M. G. Guenther, and M. A. Lazar.** 2003. A SANT motif in the SMRT corepressor interprets the histone code and promotes histone deacetylation. EMBO J. **22:**3403–3410.